Light squeezing at the transition to quantum chaos

Kirill N. Alekseev[1,2,*] and Jan Peřina[3,†]
[1]*Department of Physics, Åbo Akademi, SF-20500 Åbo, Finland*
[2]*Theory of Nonlinear Processes Laboratory, Kirensky Institute of Physics, Russian Academy of Sciences, Krasnoyarsk 660036, Russia*
[3]*Department of Optics and Joint Laboratory of Optics, Palacký University, 17 listopadu 50, 772 07 Olomouc, Czech Republic*
(Received 10 September 1997; revised manuscript received 5 December 1997)

We investigate theoretically the dynamics of squeezed state generation in nonlinear systems possessing a transition from regular to chaotic dynamics in the limit of a large number of photons. As an example, the model of a kicked Kerr oscillator is considered. We show that at the transition to quantum chaos the maximum possible degree of squeezing increases exponentially in time, in contrast to the regular dynamics, where the degree of squeezing increases only powerwise in time. We demonstrate the one-to-one correspondence of the degree of squeezing and the value of the local Lyapunov instability rate in the corresponding classical chaotic system. [S1063-651X(98)12203-1]

PACS number(s): 05.45.+b, 42.50.Dv, 03.65.Sq

I. INTRODUCTION

In recent years, it was realized that chaos can have useful applications. Among others we mention the diffusive ionization of a hydrogen atom by a microwave field [1–3], the dissociation of polyatomic molecules by laser radiation due to the transition to chaos [4,5], the stabilization of chaotic laser radiation [6] by the controlling chaos method [7], secret communications [8] using synchronization of chaotic systems [9], and the fact that chaos can be used in the generation of music variations and other sequences of context-dependent symbols [10]. All the applications mentioned dealt with classical chaos.

Recently the main activity in chaos has been shifting to the studies of quantum chaos, particularly in the behavior of quantum systems that are chaotic in the classical limit [11–16]. As a rule, quantum effects distort or suppress ''useful'' manifestations of classical chaos. For example, in the most studied system, a hydrogen atom in a microwave field, quantum effects suppress diffusive ionization by the mechanism of quantum localization [17] (the analog of Anderson localization in a solid state [18]) or by the appearance of ''scars'' of a wave function [19] in the vicinity of classical unstable periodic orbits of the corresponding classical model of the atom [20]. The only probable useful application known to us (in particular in the area of quantum optics) for quantum chaos is the suggestion [21] to utilize the effect of wave function localization in a one-dimensional quantum chaotic system driven by a periodic external field, for the generation of an electromagnetic field in the Fock state.

In this paper we discuss the possibility of generating squeezed states of the light [22–25] at the transition to quantum chaos. We show that the maximal possible degree of squeezing, achievable during some time interval of measurement, for chaotic dynamics is much greater than for regular dynamics during the same time interval. We find a direct correlation between the degree of squeezing and the value of the local Lyapunov instability rate in the corresponding classical chaotic system.

Our consideration [26] is based on three simple but general ideas.

(i) A free electromagnetic field is in a coherent state that is a Gaussian wave packet. A wave packet spreads when it propagates through a nonlinear medium. However, there still exists a time interval of well-defined quantum-classical correspondence during which the wave packet follows a path in phase space closed to the path defined by (semi)classical equations of motion. During this time interval, localized the wave packet demonstrates squeezing in one direction of phase space and stretching in another direction. As a result, one of the field quadrature components may be observed in the squeezed state at some time moments. Due to the presence of the local strong (exponential) instability inherent in the underlying classical chaotic dynamics [31], *the stretching and squeezing of the wave packet for quantum chaos is much stronger than for the case of the regular and stable dynamics*, when the distance between two initially closed trajectories in phase space increases in time only in a powerwise way [31].

(ii) The time interval of the quantum-classical correspondence depends on the number of quanta involved in the nonlinear dynamics: It has a power dependence on the number of quanta for regular dynamics and this dependence is logarithmic for chaotic dynamics [32,11,16]. In spite of the time interval of the localized wave-packet motion, when enhanced squeezing is expected, for chaotic dynamics that may be very short, this time scale is quite observable in modern experiments on light squeezing [22–25], where the average number of photons N involved in the nonlinear interaction is as great as 10^3-10^{12}. Moreover, in the conditions of the experiments, the time of the localized wave-packet motion and the well-defined quantum-classical correspondence may be of the same order as the time scale when dissipation and other factors restricting squeezing could be neglected.

(iii) Along with stretching and squeezing, another inher-

*Electronic addresses: kna@iph.krasnoyarsk.su and kna@vist.krascience.rssi.ru
†Electronic address: perina@optnw.upol.cz

ent characteristic of chaos in bounded phase space is folding. For strong chaos there are strong and multiple foldings of the wave packet; therefore, the time intervals of squeezing become very short and squeezing even becomes unstable [28]. However, at the same time that strong folding appears, the wave packet becomes delocalized and well-defined quantum-classical correspondence, which we understand here as the motion of a wave-packet center along a classical trajectory, is broken [33]. Therefore, if one studies the dynamics of the wave packet only on a time scale of well-defined quantum-classical correspondence, the squeezing could be strong and still rather stable for not very strong chaos or even for regular trajectories lying in phase space near the chaotic region.

It is already known that light squeezing can be increased near the bifurcation points between different dynamical regimes [34,25]. In addition to well-studied parametric media [34], such an increase of squeezing was predicted also for the interaction of the field with two-level atoms inside a high-Q cavity [35,36]. The explanation of enhanced squeezing near the bifurcation point has been used [37] and it is very similar to the arguments presented above that utilize quantum chaos for large squeezing: At the transition (bifurcation) between different dynamic regimes, there should exist some diverging variable and then the conjugate variable should be strongly squeezed. In spite of the similarity, our suggestion has two significant differences. First, all papers devoted to the study of enhanced squeezing in the vicinity of the instability threshold [25,34–36] dealt with the integrable or near-integrable systems with *regular dynamics*. Instead, we suggest the use of the transition from *regular* to *chaotic* dynamics. Second, from the general viewpoint, the transition to chaos and chaos itself are frequent phenomena and, as a rule, they take place for a rather wide region of control parameters, in contrast to a commonly narrow region of the control parameter characterizing a bifurcation between different regimes of regular motion.

In this paper we consider the squeezed light generation by nonlinear nonintegrable optical systems obeying the transition from regular to chaotic dynamics in the classical limit. As for other problems of quantum chaos [11–16], we deal with the semiclassical limit when a great number of quantum levels $N \gg 1$ are involved in the dynamics. Our consideration is valid for any nondissipative quantum system with $1\frac{1}{2}$ degrees of freedom, but we demonstrate our main results on the enhanced squeezing for some particular model of the nonintegrable optical system: the nonlinear oscillator periodically forced by the classical field. To investigate the nonlinear dynamics of the systems and the dynamics of squeezing in the semiclassical limit, it is natural to use the cumulant expansion technique [38] as a variation of the general $1/N$-expansion method [39]. In this paper, we use the $1/N$-expansion method suggested in [36], which is well adapted for the problems of quantum optics. We show that as long as the wave packet is localized, its dynamics may be well described by the behavior of the mean values accounting for quantum corrections and the lowest-order quantum cumulants. We demonstrate that the equations of motion for the second-order cumulants are essentially the same as those used in the definition of the Lyapunov exponent for the corresponding classical system. This allows us to find a direct correlation between the degree of light squeezing and the degree of local instability in the corresponding classical system. We also compare our approach with the generalized Gaussian approximation [23,38], which is used to find approximate solutions of many problems of quantum optics [40–42], as well as with a similar variation of the cumulant expansion [43] and find good agreement with minor differences.

Our presentation is organized as follows. In Sec. II, using the $1/N$-expansion method and starting from the Heisenberg equations of motion, we derive the self-consistent set of equations for the mean values and second-order cumulants describing the dynamics of quantum fluctuations in the semiclassical limit for an arbitrary quantum system with $1\frac{1}{2}$ degrees of freedom. We show that these equations coincide with the equations used for the calculation of the classical Lyapunov exponent. In Sec. III we discuss the conditions of validity of our basic equations for regular and chaotic dynamics and compare our approach with the results of other semiclassical techniques used in both quantum optics and quantum chaos studies. We consider the dynamics of light squeezing at the transition to quantum chaos, and compare it with the dynamics of squeezing for regular and stable motion in Sec. IV. We illustrate our results on enhanced squeezing at the transition to chaos in the model of a kicked quantum oscillator in Sec. V. Our conclusions are summarized in Sec. VI.

II. SEMICLASSICAL DYNAMICS OF QUANTUM FLUCTUATIONS: GENERAL FORMALISM

We begin with a single-mode quantum system described by the Hamiltonian $H(b,b^\dagger,t)$ including an explicit dependence on time, where b and $b^\dagger$ are Bose operators ($[b,b^\dagger]=1$) of the mode. We use normal ordering of operators. Let our system include some large parameter $N \gg 1$. The parameter N may represent the number of quanta (photons) pumped to the system [30] or the number of degrees of freedom of a quantum system [36]. Because we are interested in semiclassical limit $N \to \infty$, it is useful to introduce new operators for the annihilation and creation of photons

$$a = b/N^{1/2}, \quad a^\dagger = b^\dagger/N^{1/2} \tag{1}$$

with the commutation relation

$$[a,a^\dagger] = 1/N. \tag{2}$$

In the classical limit ($N \to \infty$), one has two commuting c numbers. The natural quantum states for the consideration of the quantum system in the semiclassical limit are coherent states [11,39]. Thus we suppose that our quantum system is initially in the coherent state $|\alpha\rangle = \exp(N\alpha a^\dagger - N\alpha^* a)|0\rangle$ corresponding to the mean number of quanta $\simeq N$. Following the general scheme of the $1/N$-expansion method [39,36], we rewrite the Hamiltonian H in the form

$$H = NH_N(a,a^\dagger,t), \tag{3}$$

where the Hamiltonian H_N generates the correct classical equations of motion in the classical limit $N \to \infty$. In the classical limit, the operators $a,a^\dagger$, following Eq. (2), may be considered as c numbers of order of unity and all quantum

corrections being of order of or less than $1/N$ could be treated by perturbation theory.

In order to illustrate the representation of the Hamiltonian in the form (3), consider a particular model of the nonintegrable quantum system: the nonlinear oscillator periodically driven by the classical field. In the interaction picture, the Hamiltonian has the form ($\hbar=1$)

$$H=\Delta b^{\dagger}b+\frac{\kappa}{2}b^{\dagger 2}b^{2}+\varepsilon N^{1/2}(b+b^{\dagger})F(t), \tag{4}$$

where b and $b^{\dagger}$ describe a single mode of the quantum field and κ is proportional to the third-order nonlinear susceptibility of a nonlinear medium. The last term in Eq. (4) corresponds to a coupling of the oscillator with an external, classical, periodically modulated field containing a large number of photons $N\gg 1$ [ε is a coupling constant, $F(t)$ is a periodic function of time, and Δ is a detuning of the mode frequency from the carrier frequency of the external field]. Using new operators $a,a^{\dagger}$ given in Eq. (1), the Hamiltonian (4) may be represented in the form (3) with

$$H_N=\Delta a^{\dagger}a+\frac{g}{2}a^{\dagger 2}a^{2}+\varepsilon(a+a^{\dagger})F(t), \quad g=\kappa N. \tag{5}$$

It may be shown that in the classical limit $N\gg 1$, when we have classical variables α,α^{*} instead of operators $a,a^{\dagger}$ with $|\alpha|\simeq 1$, the dependence $g\simeq N$ correctly gives the time scale of the energy oscillation for Kerr nonlinearity [44]. We will return to the study of the nonlinear oscillator (4) in Sec. V.

We now turn to the general case (3) and derive the equation of motion for mean values and first-order cumulants. From the Heisenberg equations for a,a^{2} and their Hermitian conjugated equations, we have the following equations of motion for the averages over coherent states:

$$i\frac{dz}{dt}=\langle V\rangle, \tag{6a}$$

$$i\frac{d}{dt}\langle(\delta\alpha)^{2}\rangle=2\langle V\delta\alpha\rangle+\langle W\rangle, \tag{6b}$$

$$i\frac{d}{dt}\langle\delta\alpha^{*}\delta\alpha\rangle=-\langle V^{*}\delta\alpha\rangle+\langle\delta\alpha^{*}V\rangle, \tag{6c}$$

where we have introduced

$$V(\alpha,\alpha^{*})=\frac{\partial H_N}{\partial a^{\dagger}}, \quad W(\alpha,\alpha^{*})=\frac{1}{N}\frac{\partial V}{\partial a^{\dagger}} \tag{7}$$

and $z\equiv\langle a\rangle$, $\delta\alpha\equiv a-z$, $\langle(\delta\alpha)^{2}\rangle\equiv\langle a^{2}\rangle-\langle a\rangle^{2}$, and $\langle\delta\alpha^{*}\delta\alpha\rangle\equiv\langle a^{\dagger}a\rangle-\langle a^{\dagger}\rangle\langle a\rangle$. In the derivation of Eqs. (6) we used the equalities [45]

$$[a,M(a,a^{\dagger})]=\frac{1}{N}\frac{\partial M}{\partial a^{\dagger}}, \quad [M(a,a^{\dagger}),a^{\dagger}]=\frac{1}{N}\frac{\partial M}{\partial a}, \tag{8}$$

which are valid for an arbitrary function M of operators $a,a^{\dagger}$ [Eq. (2)].

The set of equations (6) is not closed and actually is equivalent to the infinite-hierarchy dynamical system for moments and cumulants. To truncate it we make the substitution $a\to z+\delta\alpha$, where at least initially the mean $z\simeq 1$ and the quantum correction $|\delta\alpha(t=0)|\simeq N^{-1/2}\ll 1$. We expand functions $V(\alpha,\alpha^{*})$ and $W(\alpha,\alpha^{*})$ around the mean value $z\equiv\langle\alpha\rangle$,

$$V=V_z+\left(\frac{\partial V}{\partial\alpha}\right)_z\delta\alpha+\left(\frac{\partial V}{\partial\alpha^{*}}\right)_z\delta\alpha^{*}+\cdots,$$

$$W=W_z+\left(\frac{\partial W}{\partial\alpha}\right)_z\delta\alpha+\left(\frac{\partial W}{\partial\alpha^{*}}\right)_z\delta\alpha^{*}+\cdots, \tag{9}$$

where the subscript z means that the values of V, W, and their derivatives are calculated at mean values z and z^{*}. Substituting expansions (9) into Eqs. (6) and taking into account the equality

$$\left\langle\frac{\partial V}{\partial\alpha}\right\rangle=\left\langle\frac{\partial^{2}H_N}{\partial\alpha\partial\alpha^{*}}\right\rangle=\left\langle\frac{\partial V^{*}}{\partial\alpha^{*}}\right\rangle \tag{10}$$

resulting from Eqs. (7), we have in the first order of $1/N$ the self-consistent set of equations for mean values and first-order cumulants

$$i\frac{d}{dt}z=\langle V\rangle_z+q[z,z^{*},\langle(\delta\alpha)^{2}\rangle,\langle\delta\alpha^{*}\delta\alpha\rangle], \tag{11a}$$

$$i\frac{d}{dt}\langle(\delta\alpha)^{2}\rangle=2\left(\frac{\partial V}{\partial\alpha}\right)_z\langle(\delta\alpha)^{2}\rangle+2\left(\frac{\partial V}{\partial\alpha^{*}}\right)_z\langle\delta\alpha^{*}\delta\alpha\rangle+\langle W\rangle_z, \tag{11b}$$

$$i\frac{d}{dt}\langle\delta\alpha^{*}\delta\alpha\rangle=-\left(\frac{\partial V^{*}}{\partial\alpha}\right)_z\langle(\delta\alpha)^{2}\rangle+\left(\frac{\partial V}{\partial\alpha^{*}}\right)_z\langle(\delta\alpha^{*})^{2}\rangle. \tag{11c}$$

The small quantum correction $q\simeq 1/N$ involved in Eq. (11a) has the form of the second differential of V:

$$q=\frac{1}{2}d^{2}V|_z=\frac{1}{2}\left(\frac{\partial^{2}V}{\partial\alpha^{2}}\right)_z\langle(\delta\alpha)^{2}\rangle+\frac{1}{2}\left(\frac{\partial^{2}V}{\partial\alpha^{*2}}\right)_z\langle(\delta\alpha^{*})^{2}\rangle+\left(\frac{\partial^{2}V}{\partial\alpha^{*}\partial\alpha}\right)_z\langle\delta\alpha^{*}\delta\alpha\rangle. \tag{12}$$

The initial conditions for the system (11) are $\langle(\delta\alpha)^{2}\rangle(t=0)=\langle\delta\alpha^{*}\delta\alpha\rangle(t=0)=0$ and some arbitrary $z(0)$ is given, which is of the order of unity.

We now turn to the classical equations of motion. The classical limit may be obtained from Eq. (11a) by neglecting the quantum correction q of order $1/N$ and then the classical Hamiltonian equations are

$$i\frac{dz}{dt}=\frac{\partial H_N}{\partial z^{*}}\equiv V(z,z^{*}), \quad i\frac{dz^{*}}{dt}=-\frac{\partial H_N}{\partial z}\equiv -V^{*}(z,z^{*}). \tag{13}$$

Linearization of the classical equations (13) near z by means of the substitution $z \to z + \Delta\alpha (|\Delta\alpha| \ll |z|)$ gives

$$i\frac{d}{dt}\Delta\alpha = \frac{\partial V}{\partial z}\Delta\alpha + \frac{\partial V}{\partial z^*}\Delta\alpha^*,$$

$$i\frac{d}{dt}\Delta\alpha^* = -\frac{\partial V^*}{\partial z}\Delta\alpha - \frac{\partial V^*}{\partial z^*}\Delta\alpha^*, \tag{14}$$

where all derivatives are taken on the classical trajectory found from the Hamiltonian equations (13). Using the classical analog of the (10),

$$\frac{\partial V}{\partial z} = \frac{\partial V^*}{\partial z^*},$$

we have from Eqs. (14) the following equations of motion for *quadratic* variables $(\Delta\alpha)^2$ and $|\Delta\alpha|^2$:

$$i\frac{d}{dt}(\Delta\alpha)^2 = 2\frac{\partial V}{\partial z}(\Delta\alpha)^2 + 2\frac{\partial V}{\partial z^*}|\Delta\alpha|^2, \tag{15a}$$

$$i\frac{d}{dt}|\Delta\alpha|^2 = -\frac{\partial V^*}{\partial z}(\Delta\alpha)^2 + \frac{\partial V}{\partial z^*}|\Delta\alpha|^2, \tag{15b}$$

with the initial conditions

$$(\Delta\alpha)^2(0) = [\Delta\alpha(0)]^2, \quad |\Delta\alpha|^2(0) = [\Delta\alpha(0)][\Delta\alpha^*(0)], \tag{16}$$

where $\Delta\alpha(0)$ and $\Delta\alpha^*(0)$ are the initial values of small deviations from the classical trajectory. We define the distance D_{cl} in classical phase space between two initially closed trajectories as

$$D_{cl}(t) = |\Delta\alpha(t)| = [(\mathrm{Re}\ \Delta\alpha)^2 + (\mathrm{Im}\ \Delta\alpha)^2]^{1/2}, \tag{17}$$

where the time-dependent quantity $|\Delta\alpha(t)|$ is determined from linearized classical equations of motion (14) or from *equivalent* equations of motion for the square of linear deviations (15). The value D_{cl} characterizes the degree of local instability in the classical system: For chaotic motion $D_{cl}(t)$ increases on average exponentially with time and for regular motion D_{cl} has only a powerwise time dependence [31]. Using $D_{cl}(t)$, one can define the largest Lyapunov exponent as

$$\lambda = \lim_{t\to\infty} \frac{\ln D_{cl}(t)}{t}. \tag{18}$$

If $\lambda > 0$, the motion is chaotic and $\lambda = 0$ for regular motion [31].

We turn again to the quantum dynamics. It is easy to see that the equations of motion (11b) and (11c) for the cumulants are the same as the classical equations (15), except for the appearance of the nonlinear function $W(z,z^*)$ in Eq. (11b), which makes the cumulant equations (11b) and (11c) nonlinear. However, this difference may be overcomed by introducing the new variables

$$B = N\langle \delta\alpha^* \delta\alpha\rangle + \frac{1}{2}, \quad C = N\langle (\delta\alpha)^2\rangle, \tag{19}$$

where B is real and C is complex. Using Eqs. (7), the quantum equations of motion (11) may be rewritten in variables (19) in the form

$$i\dot{z} = \langle V\rangle_z + \frac{1}{N}Q(z,z^*,B,C,C^*), \tag{20a}$$

$$Q(z,z^*,B,C,C^*) = \frac{1}{2}\left(\frac{\partial^2 V}{\partial\alpha^2}\right)_z C + \frac{1}{2}\left(\frac{\partial^2 V}{\partial\alpha^{*2}}\right)_z C^* + \left(\frac{\partial^2 V}{\partial\alpha^*\partial\alpha}\right)_z \left(B - \frac{1}{2}\right), \tag{20b}$$

$$i\dot{C} = 2\left(\frac{\partial V}{\partial\alpha}\right)_z C + 2\left(\frac{\partial V}{\partial\alpha^*}\right)_z B, \tag{20c}$$

$$i\dot{B} = -\left(\frac{\partial V^*}{\partial\alpha}\right)_z C + \left(\frac{\partial V}{\partial\alpha^*}\right)_z C^*, \tag{20d}$$

and the corresponding equation for $C^*(t)$ that could be obtained from Eq. (20c) by complex conjugation. Initial conditions for the system (20) are

$$B(0) = 1/2, \quad C(0) = C^*(0) = 0. \tag{21}$$

Now all variables are of the order of unity and the dependence on the small parameter $1/N$ is present explicitly only in the expression for the quantum correction to classical motion in Eq. (20a).

Compare the set of classical Hamiltonian equations (13) and equations of motion (15) for classical linear fluctuations with the equations of motion (20) for mean values and quantum cumulants. It is evident that both sets of equations have the same structure with the following principal differences. First, the quantum equations (20c) and (20d) for the cumulants, in contrast to the classical equations (15), are calculated near the mean value z and take into account the quantum correction Q [Eqs. (20a) and (20b)]. Second, it should be noticed that it is impossible to obtain the initial conditions (21) for C and B from the initial conditions for the classical equations (16). However, if one considers the case of large N, when the quantum correction is small, the quantum equations (20) are *identical to the classical equations (15) used in the definition of the maximum Lyapunov exponent*. The same conclusion on the equivalence of the equations of motion for low-order cumulants and the equations of motion arising in the definition of the Lyapunov exponent has been obtained earlier for the generalized Tavis-Cammings model in [28] and for systems with Hamiltonians consisting of the sum of kinetic and potential energies in [43].

The self-consistent system of equations (20) completely describes the dynamics of quantum fluctuations in the first order of $1/N$. We shall use these equations for the description of the dynamics of light squeezing at the transition to quan-

tum chaos in Sec. IV after a discussion of the validity of our approach and its comparison with other semiclassical methods.

III. CONDITIONS OF VALIDITY AND COMPARISON WITH OTHER APPROACHES

Here we discuss the condition of validity of the $1/N$ expansion (9) and our equations of motion (20) for the mean values and cumulants. In analogy to the classical distance (17), we introduce the ''distance'' D_q for the quantum case as

$$D_q(t)=\frac{1}{N}B^{1/2}(t)\simeq[\langle|\delta\alpha|^2\rangle]^{1/2}. \tag{22}$$

It is easy to see that D_q coincides with the ''convergence radius'' $r=[\mathrm{Re}(\delta\alpha)]^2+[\mathrm{Im}(\delta\alpha)]^2$ of the $1/N$ expansion (9). Initially $D_q(0)\simeq 1/N\ll 1$, and if $D_q(t)\ll 1$ during some time interval, then the $1/N$ expansion is well defined in this time interval.

When the quantum correction in Eq. (20a) is small, Eqs. (20) are identical to the classical equations (15) arising in the definition of the classical Lyapunov exponent (18). Thus, for classically chaotic motion, we have exponential growth of $B(t)$, $C(t)$, and $D_q(t)$ as

$$D_q(t)\simeq D_q(0)\exp(\lambda\omega_0 t), \tag{23}$$

where λ is the Lyapunov exponent and ω_0 is the characteristic frequency in the classical dynamic system. For example, $\omega_0=g$ in the model of the Kerr oscillator (5). From the conditions $D_q(t)\ll 1$ and $D_q(0)\simeq 1/N$, we have the following estimate for the time scale of validity of our semiclassical approach:

$$t\ll t^*=\frac{1}{\lambda\omega_0}\ln N. \tag{24}$$

In contrast, for classically regular motion $D_q(t)$ increases with time only powerwise: $D_q(t)\simeq t^{\gamma}$, where the index $\gamma\simeq 1$ depends on the system under study. For example, $\gamma=1$ for the nonlinear oscillator with the Hamiltonian (5) for $\varepsilon=0$, as well as for integrable nonlinear oscillators with powerwise higher-order nonlinearity [46]. As a result, the time scale of validity of our approach in the case of regular motion is

$$t\ll t^*=\omega_0^{-1}N^{1/\gamma} \tag{25}$$

and it is much greater than Eq. (24) for chaotic motion. The time scale t^* has a very simple physical meaning: During the time interval t^* we have a localized wave packet with the center moving along the classical path.

The scale (24) of the well-defined quantum-classical correspondence for chaotic systems was introduced in [32] and now it is investigated in detail in different systems (for a review see [16]). The time scale (24) is very short for small N. However, under the conditions of modern experiments on light squeezing, where the average number of photons N involved in the nonlinear interaction is 10^3-10^{12}, t^* is of the order of $10-100$ of the system's characteristic periods ω_0^{-1} and thus it looks quite reasonable.

We now compare our approach to the description of the dynamics of quantum fluctuations with that widely used in quantum optics and called the generalized Gaussian approximation [23,38,40–42]. This approximation also assumes the existence of a well-localized, almost Gaussian wave packet throughout the quantum evolution. More precisely, the generalized Gaussian approximation consists in an assumption that the Fourier transform of the quantum distribution function, i.e., the quantum characteristic function, is Gaussian for any moment of time [38]. Such a quantum state corresponds to the superposition of the coherent signal and small quantum noise [23]. For such a state, only the first- and second-order cumulants are nonzero. It possesses the expression for higher-order cumulants in terms of only the first- and second-order cumulants and truncation of an infinite-hierachy dynamic system for cumulants is possible.

We compare our system (20) with the dynamic equations for the mean values and cumulants obtained within the generalized Gaussian approximation for several popular models of quantum optics: second-harmonic generation described by the Hamiltonian

$$H=\omega_1 b_1^{\dagger}b_1+\omega_2 b_2^{\dagger}b_2-(\kappa b_1^2 b_2^{\dagger}+\mathrm{H.c.}),\quad [b,b^{\dagger}]=1,$$
$$\omega_2=2\omega_1, \tag{26}$$

the problem of nondegenerate optical three-wave mixing described by the Hamiltonian

$$H=\sum_{j=1}^{3}\omega_j b_j^{\dagger}b_j-(\kappa b_1 b_2 b_3^{\dagger}+\mathrm{H.c.}),\quad \omega_3=\omega_1+\omega_2, \tag{27}$$

and the periodically forced nonlinear oscillator with the Hamiltonian (4). Considerations of these problems within the generalized Gaussian approximation are presented in Refs. [40–42]. For the forced nonlinear oscillator, we found that our self-consistent set of equations (11) and (12) coincides with the corresponding basic equations of [42] up to terms of the order of $1/N^2$, and for the problems of nondegenerate and degenerate optical three-wave mixing, our approach gives equations that are identical to the corresponding equations of motion obtained within the generalized Gaussian approximation [40,41,47].

We turn now to the discussion of squeezing at the transition from regular to chaotic motion.

IV. SQUEEZING AT THE TRANSITION TO QUANTUM CHAOS

Define the general field quadrature as $X(\theta)=a\exp(-i\theta)+a^{\dagger}\exp(i\theta)$, where θ is a local oscillator phase. A state is said to be squeezed if there is some phase θ for which the variance of X_θ

$$\langle(\delta X)^2\rangle=\langle(\delta\alpha)^2\rangle\exp(-i2\theta)+\langle(\delta\alpha^*)^2\rangle\exp(i2\theta)$$
$$+2\langle|\delta\alpha|^2\rangle+1/N \tag{28}$$

is less than the variance for coherent state or the vacuum [22]. In variables (19), the condition of squeezing takes the form

$$S(\theta)=2B+C\exp(-i2\theta)+C^{*}\exp(i2\theta)<1. \quad (29)$$

The minimum of the variance of the general field quadrature (29) with respect to its dependence on the local oscillator phase θ is reached at θ_{min}, determined as

$$\theta_{min}=(\varphi-\pi)/2, \quad (30)$$

where φ is the argument of the cumulant $C[C\equiv|C|\exp(i\varphi)]$. For $\theta=\theta_{min}$, the condition of squeezing (29) is

$$S\equiv S(\theta_{min})=2(B-|C|)<1. \quad (31)$$

The value S determines the minimum half axis of the quantum noise ellipse [23]. The condition (31) is called *principal squeezing* because it gives the maximum squeezing measurable by homodyne detection [48,23].

Let us now compare the dynamics of the principal squeezing for classically regular and chaotic motion. Initially the Gaussian wave packet spreads when it propagates through a nonlinear medium. However, there still exists the time interval of the well-defined quantum-classical correspondence (24) or (25) during which the wave packet's center follows a path in phase space governed by the semiclassical equation of motion (20a). Moreover, because our equations of motion for cumulants (20c) and (20d) in fact coincide with the equations arising from the definition of the maximum Lyapunov exponent, we can apply simple physical arguments to the strong deformation of the classical phase volume at chaos for the prediction of the strong squeezing of the noise ellipse at quantum chaos in the semiclassical limit.

Due to the presence of the strong (exponential) local instability inherent in the underlying classical chaotic dynamics, a quantum noise ellipse may be strongly stretched in one direction and squeezed in another direction. As a result, the value of principal squeezing S in Eq. (31), which correlates with the minimum half axis of the quantum noise ellipse, on average exponentially decreases in time

$$S(t)\simeq\exp(-\lambda\omega_0 t). \quad (32)$$

The stretching and squeezing of a noise ellipse at quantum chaos is much stronger than for the case of regular and stable dynamics, when the distance between two initially closed trajectories in phase space increases in time in a powerwise way resulting in only a powerwise decrease of the principal squeezing in time

$$S(t)\simeq(\omega_0 t)^{-\beta}, \quad (33)$$

where the constant $\beta\simeq 1$. As an example of such a time dependence, we consider the Kerr oscillator (5) without an external field ($\varepsilon=0$). In this case the model is integrable, and from an exact solution in the limit $N\gg 1$ [49], we get

$$S(t)=1+2|\alpha_0|^2 gt[|\alpha_0|^2 gt-(1+|\alpha_0|^4 g^2 t^2)^{1/2}]$$
$$\rightarrow(6|\alpha_0|^2 gt)^{-1}, \quad gt\gg 1 \quad (34)$$

where α_0 is some initial condition ($|\alpha_0|\simeq 1$). The same result could be obtained directly from our semiclassical approach neglecting the quantum correction in Eq. (20) and combining it with Eq. (31) [46].

Making a comparison of squeezing for regular and chaotic motion, several comments are necessary.

(i) Both formulas (32) and (33) are obtained within the pure classical picture when quantum corrections are neglected. The deviations from dependences (32) and (33) are expected when quantum corrections become sufficient, especially at $t\simeq t^{*}$.

(ii) Squeezing for chaotic dynamics is exponential only on average. Actually, the rate of phase volume deformation and, consequently, the rate of quantum noise ellipse deformation and squeezing are directly related in the semiclassical limit ($N\gg 1$) to the degree of local Lyapunov instability D_q [Eq. (22)] in the system, which at some moments in time may be different from the maximum Lyapunov exponent (18) measured at asymptotics $t\rightarrow\infty$. Such behavior is typical, for instance, for a chaotic trajectory that spends some time near a stable island. In this case, the local instability and statistical properties of chaotic motion are weak [50]. Finally, the trajectory escapes to a large chaotic sea and the local instability becomes strong. Of course, the Lyapunov exponent is positive in both cases. Formally, the resulting nonmonotonic dependence of squeezing on time could be modeled by a slowly varying dependence of the parameter λ [Eq. (32)]. We will discuss this problem further in Sec. V.

(iii) In addition to the wide class of integrable systems with stable regular dynamics, there is a small class of systems with regular but unstable dynamics, for which the distance D_q given in Eq. (22) increases in time exponentially. In such a case the systems are in the state near the bifurcation point between different dynamic behaviors and they are exponentially unstable. The mechanism of enhanced squeezing in unstable systems with regular dynamics is very similar to that discussed at the transition to quantum chaos, and has been discussed in detail in [34–37].

(iv) Considering squeezing at chaos, we have not discussed yet the influence of one of the main characteristics of chaos: folding of the phase volume that, in addition to stretching, is present in any bounded Hamiltonian system. For strong chaos, strong and multiple folding of the phase volume appears during the time scale of the well-defined quantum-classical correspondence. The perimeter of the phase volume increases in time exponentially and eventually the phase volume envelope gets some fractal-like structure [31]. Moreover, the final shape of the phase volume is very sensitive to small changes of the initial conditions and/or parameters. The complex and unstable evolution of the phase volume is displayed in the time dependence of squeezing [28]. For strong chaos and long enough time, squeezing becomes strongly dependent on tiny variations of the system's parameters. Such a regime of squeezing was called in [28] *unstable squeezing*. For unstable squeezing, the range of the local oscillator phase, for which squeezing is possible, becomes so narrow that it makes observation of squeezing practically impossible [28].

It should be noticed that at the same time when multiple folding of wave packet appears, the quantum-classical correspondence breaks down. For strong chaos this time scale is

very short. In contrast, for weak chaos, the time scale of the well-defined quantum-classical correspondence and time scale of strong folding may be rather long in the semiclassical limit, resulting in stable and enhanced squeezing. The same arguments should be valid for regular trajectories located near the chaotic motion in phase space. Actually, during a finite time interval stability properties of a given trajectory are determined by the time dependence of the distance (17) or (22) between two initially nearby trajectories. At a finite time the value of D_q for the regular trajectory is often practically indistinguishable from the nearby chaotic trajectory [51] resulting in the same degree of squeezing. We will illustrate a general picture of squeezing at the transition to quantum chaos through an example of the model of the kicked nonlinear oscillator in Sec. V.

Concluding this section, let us compare qualitatively the maximum achievable degree of principal squeezing for regular and chaotic motion during the time interval of the well-defined quantum-classical correspondence. First consider the case of squeezing at chaos. Principal squeezing on average is exponential (32), and at the end of time interval (24) it should be not less than $S(t^*)\simeq\exp(-\lambda\omega_0 t^*)\simeq 1/N$. For regular dynamics, the principal squeezing has a powerwise time dependence (33) and it should be not less than $S(t^*)\simeq(\omega_0 t^*)^{-\beta}\simeq N^{-\beta/\gamma}$, where constants $\gamma\simeq 1$ and $\beta\simeq 1$, and we used the estimate (25) of t^* for regular motion. Thus these rough estimates show that the degree of squeezing at time t^* is comparable in the cases of regular and chaotic dynamics, but because t^* is much shorter for chaotic dynamics than for regular, squeezing is much faster in the chaotic systems.

V. EXAMPLE: THE KICKED NONLINEAR OSCILLATOR

Consider a nonlinear oscillator interacting with a time-periodic field as given in Eqs. (4) and (5). This model describes, for example, a high-Q cavity filled by a medium with Kerr nonlinearity and excited by an external laser field [21]. The same effective Hamiltonian may also govern the interaction of a laser field with a high-density exciton in a semiconductor [52]. The different variations of the model discussed are very popular in both quantum optics [53] and quantum chaos [11,42,54] studies.

In this paper we choose the form of $F(t)$ in Eq. (5) as a periodic sequence of kicks

$$\delta_T(t)=\sum_{n=-\infty}^{\infty}\delta(t-nT), \tag{35}$$

where $\delta(t)$ is the Dirac delta function. In an experiment, a sequence of short light pulses can be generated by a mode-locked laser. The use of the sequence of kicks is used to obtain discrete maps instead of differential equations and it sufficiently simplifies computations and reduces numerical errors, which is especially important when we analyze the influence of small quantum corrections ($N\gg 1$) on the dynamics of squeezing.

In what follows we shall use scaled variables $t'=gt$ and $\Delta'=\Delta/g$ measuring time and detuning in the units of the coupling constant g and then we omit primes, which is formally equivalent to choosing $g\equiv 1$ in the Hamiltonian (5). The classical equation of motion (13) obtained from the Hamiltonian (5) has the form

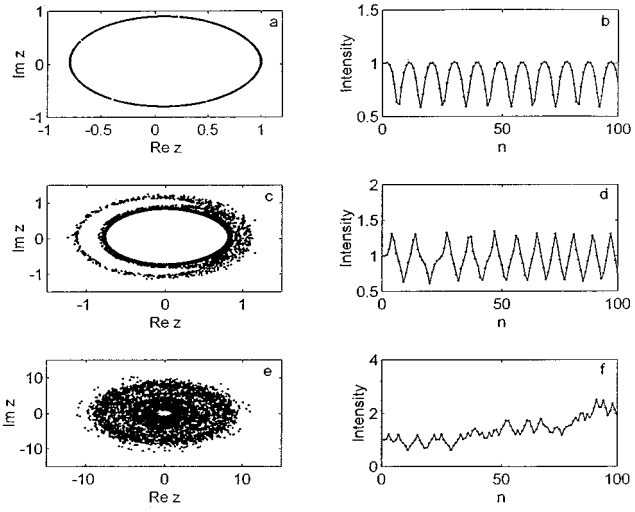

FIG. 1. Nonlinear dynamics of the kicked classical nonlinear oscillator ($N\to\infty$): phase portrait and time dependence of the intensity $|z_n|^2$ for (a) and (b) the regular behavior at $T=3$, (c) and (d) weak chaos at $T=6.4$, and (e) and (f) hard chaos at $T=10$. The initial condition is $z_0=1$; $\varepsilon=0.1$ and $\Delta=1$. Time is measured in the number of kicks.

$$i\frac{dz}{dt}=\Delta z+g|z|^2z+\varepsilon\,\delta_T(t). \tag{36}$$

From Eq. (36) and using a standard technique [11,31], we have the classical map

$$z_{n+1}=F(z_n),\quad F(z_n)=\exp[-iT(\Delta+|z_n-i\varepsilon|^2)](z_n-\varepsilon), \tag{37}$$

where z_n is the value of z just before nth kick, $z_n\equiv z(nT-0)$. It may be shown analytically [54] that the approximate criterion of the transition from regular motion to strong and global chaos for the map (37) in the limiting case $\varepsilon\ll 1$ is

$$K=2\varepsilon T\gtrsim 1. \tag{38}$$

We illustrate the dynamics governed by the map (37) in Fig. 1, where phase portraits [Fig. 1(a), 1(c), and 1(e)] and the time dependence of intensity $|z_n|^2$ [Figs. 1(b), 1(d), and 1(f)] are shown for the cases of regular motion, weak chaos, and strong chaos correspondingly.

We now turn to the dynamics of quantum cumulants and the mean values with quantum corrections. Using the smallness of $1/N$, we obtain from the semiclassical equations of motion (20) and the classical map (37) the following coupled maps describing the dynamics of mean values and cumulants (details of the derivation of these maps are presented in the Appendix):

$$z_{n+1}=F(z_n)+\frac{1}{N}Q_n, \tag{39a}$$

$$C_{n+1}=\exp[-i2T(\Delta+|z_n-i\varepsilon|^2)]\{-2(z_n-i\varepsilon)^2 \times(T^2|z_n-i\varepsilon|^2+iT)B_n+(1-2iT|z_n-i\varepsilon|^2)C_n -T^2(z_n-i\varepsilon)^2[(z_n-i\varepsilon)^2C_n^*+\text{c.c.}]\}, \tag{39b}$$

$$B_{n+1}=(2T^2|z_n-i\varepsilon|^4+1)B_n+T^2|z_n-i\varepsilon|^2[(z_n-i\varepsilon)^2C_n^* +\text{c.c.}]+[-iT(z_n-i\varepsilon)^2C_n^*+\text{c.c.}], \tag{39c}$$

where $F(z_n)$ in Eq. (39a) is the classical map introduced in Eq. (37) and the quantum correction Q_n in Eq. (39a) has the form

$$Q_n=A_1(z_n,z_n^*)C_n+A_2(z_n,z_n^*)C_n^*+A_3(z_n,z_n^*)(B_n-1/2), \tag{40a}$$

$$A_1(z_n,z_n^*)=\frac{1}{2}e^{-iT(\Delta+|z_n-i\varepsilon|^2)}[-iT(z_n^*+i\varepsilon) \times(2-iT|z_n-i\varepsilon|^2)], \tag{40b}$$

$$A_2(z_n,z_n^*)=\frac{1}{2}e^{-iT(\Delta+|z_n-i\varepsilon|^2)}[-T^2(z_n-i\varepsilon)^3], \tag{40c}$$

$$A_3(z_n,z_n^*)=-e^{-iT(\Delta+|z_n-i\varepsilon|^2)}T(z_n-i\varepsilon)(T|z_n-i\varepsilon|^2+2i). \tag{40d}$$

Following Eq. (21), the initial conditions for the maps (39) are $B_0=1/2$, $C_0=0$, and arbitrary z_0 of order unity. The self-consistent set of maps (39) and (40) determines the dynamics of the quantum fluctuations for the kicked nonlinear oscillator in first order of $1/N$.

Now we want to compare the time dependence of the principal squeezing S in Eq. (31), the degree of local instability (22), and the quantum correction Q in Eq. (40) for three characteristic cases of classical dynamics: regular motion, mild chaos, and hard chaos. To avoid the dependence of D_q on N it is useful to introduce the new normalized distance

$$d=ND_q.$$

Phase portraits and time dependences of the intensity $|z|^2$ for the three characteristic cases of classical dynamics governed by the map (37) are shown in Fig. 1. The time dependences of $\log_{10}S$, $\log_{10}d$, and $\log_{10}Q$ for a large but finite number of quanta $N=10^9$ are shown in Fig. 2, where curves 1, 2, and 3 correspond to the cases of regular motion ($\lambda=0$) and chaotic motion with an increasing value of the Lyapunov exponent λ, respectively. As is evident from a comparison of Figs. 2(a) and 2(b), the strongest local instability determines the highest degree of squeezing. It should be mentioned that the difference in the magnitude of principal squeezing for chaotic motion and regular motion is of several orders during only several kicks. A powerwise time dependence of d [Fig. 2(b), curve 1] is assisted by the corresponding slow growth in time of the quantum correction [Fig. 2(c), curve 1]. In contrast, for chaotic motion, the growth of d and Q is exponential [curves 2 and 3 in Figs. 2(b) and 2(c)], resulting in a logarithmic dependence of the applicability of the semiclassical approach on the number of quanta in Eq. (24).

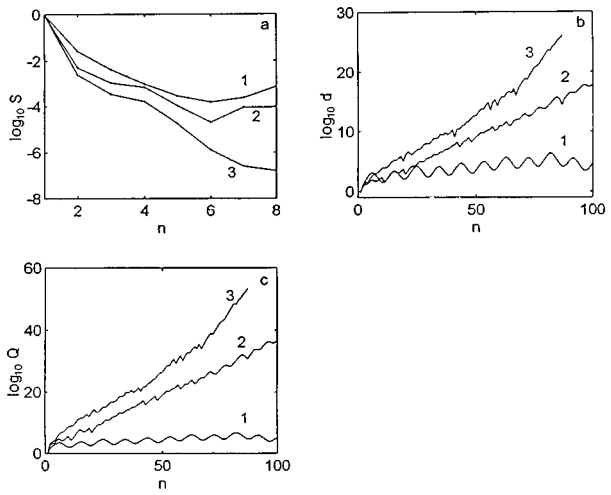

FIG. 2. Time dependence of (a) the principal squeezing, (b) the distance between two initially closed trajectories, and (c) the quantum correction to the motion of wave-packet center. Curve 1 corresponds to the regular dynamics at $T=3$, curve 2 to the mild chaos ($T=7$), and curve 3 to the hard chaos ($T=10$). The average photon number is $N=10^9$; the initial condition and other parameters are the same as in Fig. 1.

The increment of local instability and the corresponding degree of squeezing are complex functions of the initial conditions or parameters. As a result, the dependence of squeezing on initial conditions or parameters may be rather complex. In Fig. 3 we plot the minimum value min $\log_{10}S$ of the principal squeezing during seven kicks and the degree of local instability $\log_{10}d$ as a function of the kick's period T at fixed initial conditions, $\varepsilon=0.1$, and number of quanta $N=10^9$. The regions of parameter values with mainly regular

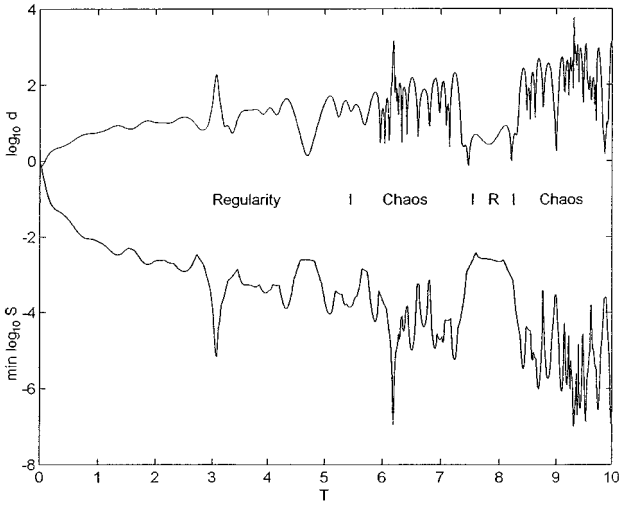

FIG. 3. In the upper part of the figure, the logarithm of the distance between two initially closed classical trajectories $\log_{10}d$ after seven kicks is plotted as a function of kicking period T defined in dimensionless units (see the text). In the lower part, the minimum of the logarithm of the principal squeezing min $\log_{10}S$ during seven kicks as a function of the kick period T is plotted for the average photon number $N=10^9$. In the center of the figure, big intervals of T with primary regular and primary chaotic behavior are marked. The amplitude of perturbation and detuning are fixed: $\varepsilon=0.1$ and $\Delta=1$. The initial condition is the same as in Fig. 1.

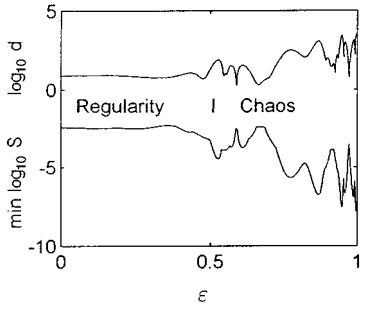

FIG. 4. Local Lyapunov rate $\log_{10}d$ after nine kicks and the minimum of principal squeezing during nine kicks as functions of dimensionless perturbation amplitude ε at fixed $T=1$. Other parameters are the same as in Fig. 3.

or chaotic motion in the classical limit ($N\to\infty$) are marked in the center of the plot. The first large region of chaos begins at $T_{cr}\approx 5.4$, which is in good agreement with the approximate criterion (38) of the transition to chaos. Of course, there are some singular values of the parameter T corresponding to regular motion in the range of T that is mainly filled by chaotic trajectories.

As is evident from Fig. 3, there is a direct correlation between the degree of squeezing and the degree of instability $\log_{10}d$. Because we present the dependences of $\log_{10}d$ and squeezing on T for only seven kicks, the degree of instability and squeezing may be comparable for some points from regular and chaotic ranges of T. However, generally, as it follows from Eq. (38), the degree of instability increases with increasing T and correspondingly we have an increase of squeezing (Fig. 3).

In Fig. 4 we plot $\log_{10}d$ and the minimum of $\log_{10}S$ during nine kicks as a function of another parameter ε and at fixed T and initial conditions. Again, the correlation of local instability and squeezing, and an enhancement of squeezing at the transition to chaos are visible. The same dependences but for three kicks instead of nine are shown in Fig. 5(a). In spite of the correlation between the degree of squeezing and $\log_{10}d$ it is also evident in Fig. 5(a) that the increase of squeezing at the transition from regular to chaotic motion ($\varepsilon_{cr}\approx 0.5$) is smoothed more than in the case of nine kicks shown in Fig. 4.

As we already mentioned, the degree of local instability may itself depend on time. This is illustrated in Fig. 5(b), where in an interval of $3-8$ kicks the instability for $\varepsilon=1.8$ (curve 1) is greater than for $\varepsilon=2.22$ (curve 2). As a

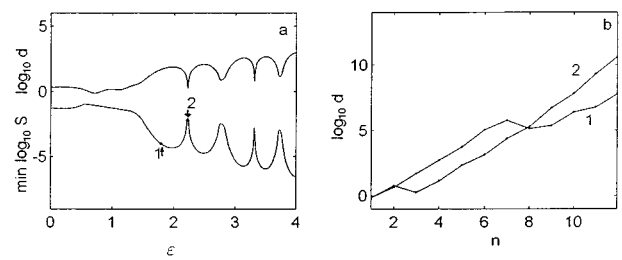

FIG. 5. (a) Same as in Fig. 4, but after only three kicks instead of nine. Point 1 corresponds to $\varepsilon=1.8$ and point 2 to $\varepsilon=2.22$. (b) Time dependence of the classical local Lyapunov rate. Curves 1 and 2 are plotted for the same values of ε as in (a) and at $T=1$.

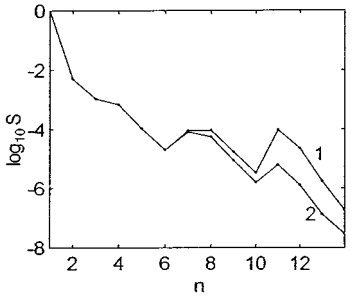

FIG. 6. Time dependence of the principal squeezing for chaotic motion ($T=7$, $\varepsilon=0.1$). Curve 1 corresponds to the classical limit $N\to\infty$ and curve 2 to $N=10^7$.

result, the squeezing during three kicks at $\varepsilon=1.8$ [point 1 in Fig. 5(a)] is greater than for $\varepsilon=2.22$ [point 2 in Fig. 5(a)]. After eight kicks we have the inverse picture: The instability for $\varepsilon=2.22$ is greater than at $\varepsilon=1.8$ [see Fig. 5(b)], resulting in enhanced squeezing for the parameter's values of point 1 in comparison to squeezing for the parameter's values of point 2.

Summarizing our findings from Figs. 3–5, we see that in the semiclassical limit the degree of squeezing has a one-to-one correspondence to the degree of local instability in the system. For a short time of the order of several kicks, the dependence of squeezing on the Lyapunov exponent, which is calculated in the limit $t\to\infty$, is not well pronounced. Moreover, squeezing for regular motion located near the border of the transition to chaos is comparable to squeezing for weak chaos. The dependence of squeezing on the value of the Lyapunov exponent becomes more pronounced for moderate times of the order of ten kicks.

We compare now the time dependence of principal squeezing for different N. The dependence of S on t at $N\to\infty$ (curve 1) and at $N=10^7$ (curve 2) is presented in Fig. 6 for the case of mild chaos. Curves 1 and 2 coincide during seven kicks, which determines the time interval of the well-defined quantum-classical correspondence for such a choice of parameters. Moreover, our numerical calculations demonstrate that if the number of quanta in two orders increases up to $N=10^9$, the squeezing is indistinguishable from squeezing at $N\to\infty$ up to 15 kicks. This finding is well explained by remembering the $\ln N$ dependence (24) of the time scale.

Thus we demonstrate that an increase in the average number of photons N results in a corresponding increase of the time interval for the applicability of our description of squeezing dynamics. On the other hand, the number of photons $N\geqslant 10^7$ initially pumped to the system is quite realistic for contemporary experiments on light squeezing [22–25].

Let us now discuss the stability of chaotic squeezing. The time dependence of the optimal local oscillator phase θ_{min} given in Eq. (30) for the cases of regular and mild chaos is shown in Fig. 7 for two slightly different initial conditions $z_0=1$ and $z_0=1.001$. The deviation of the optimal local oscillator phase values related to different z_0 in the case of regular dynamics is small throughout the time evolution presented in Fig. 7 (see the dashed and dotted curves). For chaos ($T=7$, $\varepsilon=0.1$), the deviation is sufficient only at the fifth kick (boxes and pluses in Fig. 7). Thus, for not very strong chaos, there is a time interval during which squeezing is enhanced and still stable.

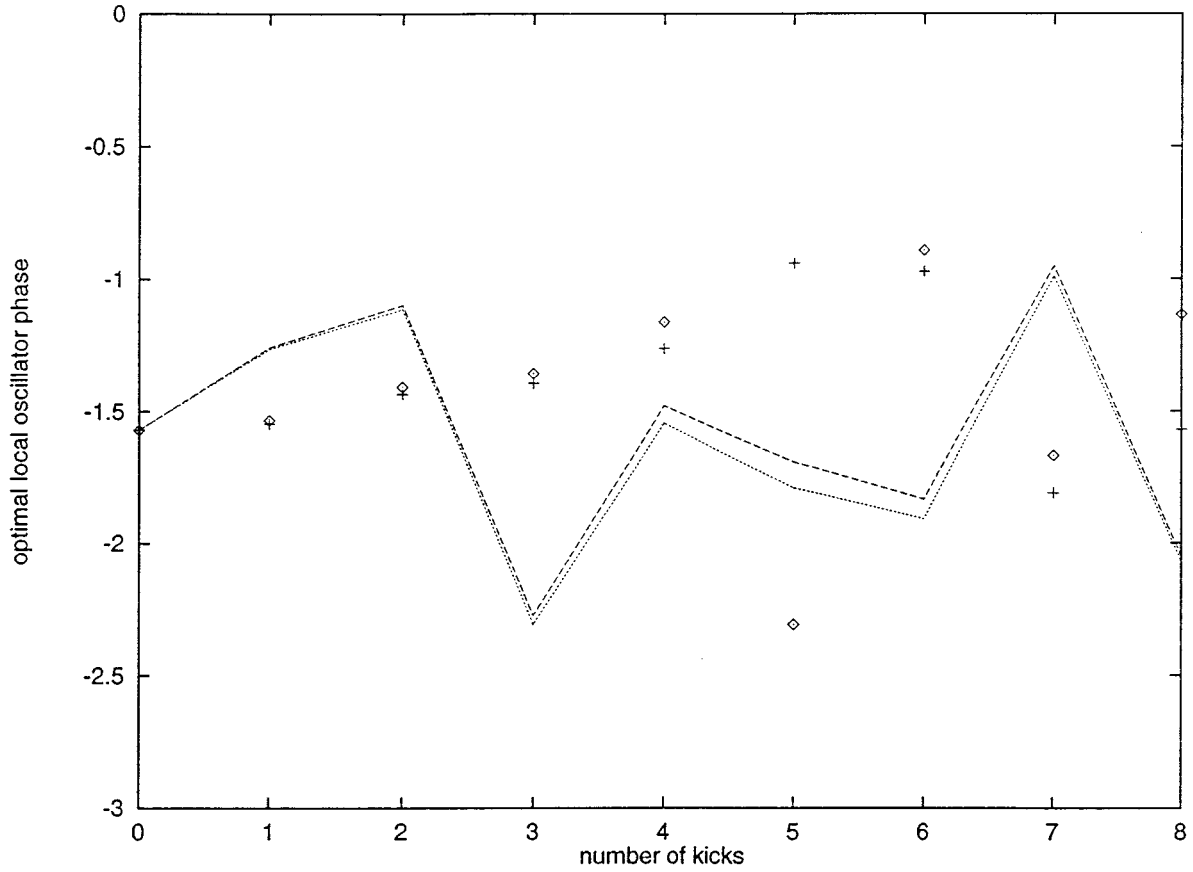

FIG. 7. Time dependence of the optimal local oscillator phase θ_{min} in the case of mild chaos at $T=7$, $\varepsilon=0.1$, and for different initial conditions: $z_0=1$ (boxes) and $z_0=1.001$ (pluses). Compare with the time dependence of θ_{min} for regular motion at $T=3$ and $\varepsilon=0.1$ shown by the dashed line for $z_0=1$ and by the dotted line for $z_0=1.001$.

VI. CONCLUSION

In Ref. [25] a fundamental question was asked: ''What is the best squeezing device?'' The answer founded in [25] is based on the fact that ''the quantum noise reduction is effective below and above the bifurcation points between dynamical regimes.'' The reason for enhanced squeezing consists in the fact that ''the same classical linearized equations are used to study the stability of the system and to calculate its quantum fluctuations'' [25]. It should be stressed that only integrable or near-integrable systems with regular dynamics were discussed in [25]. The results of our paper demonstrate that in addition to a very narrow class of integrable systems near the threshold of instability, there is another wide class of potentially ''the best squeezing devices'': systems at the transition to quantum chaos operating during the time interval of the well-defined quantum-classical correspondence.

In this paper we have presented a semiclassical theory for the quantum systems with $1\frac{1}{2}$ degrees of freedom and illustrated our findings on the model of kicked nonlinear oscillator. Direct numerical observation of enhanced squeezing in the model of a kicked quantum rotator at the transition to quantum chaos (nonperturbative approach) will be presented elsewhere [55].

ACKNOWLEDGMENTS

We would like to thank Boris Chirikov, Claude Fabre, Zdeněk Hradil, Antonín Lukš, and Vlasta Peřinová for discussions. Part of the work was done during the visit of K. N. A. to the Department of Physics, University of Illinois at Urbana-Champaign. K. N. A. thanks Professor David Campbell for hospitality. K. N. A. also thanks Professor Juhani Kurkijärvi for hospitality in Åbo. This research was partially supported by the Russian Fund for Basic Research (Grant No. 96-02-16564), INTAS (Grant No. 94-2058), Academy of Finland (Grant No. 35874), Krasnoyarsk Regional Science Foundation, Czech Grant Agency (Grant No. 202/96/0421), and the Czech Ministry of Education (Grant No. VS96028).

APPENDIX

In this appendix we briefly describe the derivation of the coupled maps (39) and (40) for the mean values and second-order cumulants. We begin with the equations for the mean values (39a). Substituting the Hamiltonian of the nonlinear oscillator (5) with $F(t)$ given in Eq. (35) by Eq. (20a) and using the smallness of the quantum correction $N^{-1}Q$, we first neglect the influence of the quantum correction and find the solution of the classical equations of motion given by the map (37) and then substitute this classical solution into the expression for the quantum correction $Q(z\rightarrow z_{cl}, z^*\rightarrow z_{cl}^*)$. Such a perturbative approach is valid during the time interval (24) of the well-defined quantum-classical correspondence for chaotic systems and the time interval (25) for systems with regular dynamics.

To find the explicit form of the quantum correction Q, we remember that it has the form of the second differential of $z(t)$ [see Eqs. (12) and (20b)]. Determining d^2z_{n+1}, we obtain the expression (40) for the quantum correction Q.

We now turn to the derivation of the maps (39b) and (39c) for cumulants B and C. As it has been shown in Sec. II, the equations of motion for B and C may be obtained by linearization of classical motion equations near the classical trajectory, taking into account the quantum correction, and by using substitutions $B\rightarrow|dz|^2$ and $C\rightarrow(dz)^2$. We adopt this finding for the derivation of maps for B and C. Utilizing again the perturbative approach, we first find the differential of the map (39a) neglecting the influence of the quantum correction

$$Dz_{n+1}=e^{-iT(\Delta+|z_n-i\varepsilon|^2)}\{-iT(z_n-i\varepsilon)[(z_n-i\varepsilon)dz_n^* + (z_n^*+i\varepsilon)dz_n]+dz_n\}. \tag{A1}$$

From Eq. (A1) we obtain the maps for quadratic variables $B_n\equiv|dz_n|^2$ and $C_n\equiv(dz_n)^2$ in the forms (39b) and (39c). Finally, we suppose that the variables z_n, z_n^* included in Eqs. (39b) and (39c) are calculated, taking into account the quantum correction, i.e., using formula (39a). The perturbative approach used in the derivation of Eqs. (39b) and (39c) is valid during the time interval of the well-defined quantum-classical correspondence when the quantum corrections to the classical equations are small. To avoid misprints we checked the expressions for our coupled maps (39) and (40) by symbolic computation in the package MATHEMATICA.

[1] For an experiment, see, J. E. Beyfield and P. M. Koch, Phys. Rev. Lett. **33**, 258 (1974); K. A. H. van Leeuwen, G. V. Oppen, S. Renwick, J. B. Bowlin, P. M. Koch, R. V. Jensen, O. Rath, D. Richards, and J. G. Leopold, *ibid.* **55**, 2231 (1985).

[2] For a theory, see, J. G. Leopold and I. C. Percival, Phys. Rev. Lett. **41**, 944 (1978); B. I. Meerson, E. A. Oks, and P. U. Sasorov, Pis'ma Zh. Éksp. Teor. Fiz. **29**, 79 (1979) [JETP Lett. **29**, 72 (1979)]; D. A. Jones, J. G. Leopold, and I. C. Percival, J. Phys. B **13**, 31 (1980).

[3] For a review see J. E. Bayfield, in *Chaos-Xaoc, Soviet-American Perspectives on Nonlinear Science*, edited by D. K. Campbell (American Institute of Physics, New York, 1990), p. 433; P. M. Koch, *ibid.*, p. 441.

[4] For an experiment see T. B. Simpson, J. G. Black, I. Burak, E. Yablonovitch, and N. Blombergen, J. Chem. Phys. **83**, 628 (1985), and references therein.

[5] For a theory see E. V. Shuryak, Zh. Éksp. Teor. Fiz. **71**, 2039 (1976) [Sov. Phys. JETP **44**, 1070 (1976); J. R. Ackerhalt and P. W. Milonni, Phys. Rev. A **34**, 1211 (1986); **34**, 5137 (1986).

[6] R. Roy, T. W. Murphy, Jr., T. D. Maier, and Z. Gills, Phys. Rev. Lett. **68**, 1259 (1992); R. Roy, Z. Gills, and K. S. Thornburg, Opt. Photonics News **5**, 8 (1994).

[7] E. Ott, C. Grebogi, and J. A. Yorke, Phys. Rev. Lett. **64**, 1196 (1990).

[8] K. M. Cuomo and A. V. Oppenheim, Phys. Rev. Lett. **71**, 65 (1993).

[9] L. M. Pecora and T. L. Carroll, Phys. Rev. Lett. **64**, 821 (1990).

[10] D. S. Dabby, Chaos **6**, 95 (1996).

[11] G. M. Zaslavsky, Phys. Rep. **80**, 175 (1981).

[12] M. Gutzwiller, *Chaos in Classical and Quantum Mechanics* (Wiley-Interscience, New York, 1991).

[13] F. Haake, *Quantum Signatures of Chaos* (Springer, Berlin, 1991).

[14] L. E. Reichl, *The Transition to Chaos: Quantum Manifestations* (Springer, Berlin, 1992).

[15] *Chaos and Quantum Physics*, Proceedings of the Les Houches Summer School of Theoretical Physics, Les Houches, France, 1989, Session LIL, edited by M. J. Giannoni, A. Voros, and J. Zinn-Justin (Elsevier, Amsterdam, 1991).

[16] G. Casati and B. V. Chirikov, Physica D **86**, 220 (1995).

[17] G. Casati, B. V. Chirikov, and D. L. Shepelansky, Phys. Rev. Lett. **53**, 2525 (1984); G. Casati, B. V. Chirikov, I. Guarneri, and D. L. Shepelansky, Phys. Rep. **154**, 77 (1987).

[18] S. Fishman, D. Grempel, and R. Prange, Phys. Rev. Lett. **29**, 1639 (1984).

[19] E. J. Heller, Phys. Rev. Lett. **53**, 1515 (1984).

[20] R. V. Jensen, M. M. Sanders, M. Saraceno, and B. Sundaram, Phys. Rev. Lett. **63**, 2771 (1989).

[21] J. R. Kuklinski, Phys. Rev. Lett. **64**, 2507 (1990).

[22] D. F. Walls and G. J. Milburn, *Quantum Optics* (Springer-Verlag, Berlin, 1994).

[23] J. Peřina, *Quantum Statistics of Linear and Nonlinear Optical Phenomena* (Kluwer Academic, Dordrecht, 1991).

[24] S. Reynaud, A. Heidmann, E. Giacobino and C. Fabre, in *Progress in Optics XXX*, edited by E. Wolf (Elsevier, Amsterdam, 1992), p. 1.

[25] C. Fabre, Phys. Rep. **219**, 215 (1992).

[26] To our knowledge, enhanced light squeezing at the transition to quantum chaos was predicted in [27]. Enhanced light squeezing at the transition to chaos in the generalized Tavis-Cummings model was studied in detail in [28]. Strong squeezing of wave packets on a time scale of well-defined quantum-classical correspondence has been discussed by B. V. Chirikov as a characteristic of quantum chaos [29] (see also Sec. 3.1 in [16]). Our present consideration of the problem is an extension of [30].

[27] K. N. Alekseev, Kirensky Institute of Physics, Russian Academy of Sciences, Report No. 674F, 1991.

[28] K. N. Alekseev, Opt. Commun. **116**, 468 (1995).

[29] B. V. Chirikov (unpublished).

[30] Kirill N. Alekseev and Jan Pěrina, Phys. Lett. A **231**, 373 (1997).

[31] A. Lichtenberg and M. Lieberman, *Regular and Stochastic Motion* (Springer-Verlag, Berlin, 1983).

[32] G. P. Berman and G. M. Zaslavsky, Physica A **91**, 450 (1978); M. Berry, N. Balazs, M. Tabor, and A. Voros, Ann. Phys. (N.Y.) **122**, 26 (1979).

[33] After delocalization of the wave packet, the quantum-classical correspondence may be defined using only a statistical description, in spite of the fact that some semiclassical tools are still

valid; see, for example, E. J. Heller and S. Tomsovic, Phys. Rev. Lett. **67**, 664 (1991); Phys. Today **46**, (7), 38 (1993).
[34] L. A. Lugiato, P. Galatola, and L. M. Narducci, Opt. Commun. **76**, 276 (1990).
[35] A. Heidmann, J. M. Raimond, and S. Reynaud, Phys. Rev. Lett. **54**, 326 (1985).
[36] A. Heidmann, J. M. Raimond, S. Reynaud, and N. Zagury, Opt. Commun. **54**, 189 (1985).
[37] A very nice discussion of strong squeezing near bifurcation points is presented in Ref. [25], Sec. 3.2.1, and references cited therein.
[38] R. Schak and A. Schenzle, Phys. Rev. A **41**, 3847 (1990).
[39] L. G. Yaffe, Rev. Mod. Phys. **54**, 407 (1982).
[40] J. Peřina, J. Křepelka, R. Horák, Z. Hradil, and J. Bajer, Czech. J. Phys. Sect. B **37**, 1161 (1987); P. Szlachetka, K. Grygiel, J. Bajer, and J. Peřina, Phys. Rev. A **46**, 7311 (1992).
[41] J. Peřina, J. Bajer, J. Křepelka, and Z. Hradil, J. Mod. Opt. **34**, 965 (1987).
[42] P. Szlachetka, K. Grygiel, and J. Bajer, Phys. Rev. E **48**, 101 (1993).
[43] B. Sundaram and P. W. Milonni, Phys. Rev. E **51**, 1971 (1995).
[44] K. N. Alekseev, G. P. Berman, A. V. Butenko, A. K. Popov, A. V. Shalaev, and V. Z. Yakhnin, J. Mod. Opt. **37**, 41 (1990).
[45] See, e.g., Section 4.1.4 in Ref. [23].
[46] K. N. Alekseev and J. Peřina (unpublished).
[47] Strictly speaking, the problem of second-harmonic generation does not belong to the class of systems (3). We analyze in this paper single-mode quantum systems with an explicit time dependence. However, the examples of second-harmonic generation and optical three-wave mixing problems demonstrate that the extension of our formalism to the case of multimode quantum models is straightforward, at least for the case of simple powerwise nonlinearity.
[48] A. Lukš, V. Peřinová, and J. Peřina, Opt. Commun. **67**, 149 (1988).
[49] R. Tanaś, A. Miranowicz, and S. Kielich, Phys. Rev. A **43**, 4014 (1991).
[50] V. V. Beloshapkin and G. M. Zaslavsky, Phys. Lett. **97A**, 121 (1983).
[51] Note that quick growth of the variance with time for regular trajectories located near chaotic trajectories has been observed in the direct numerical simulation of dynamics of very narrow wave packets in the model of a kicked quantum rotator by B. L. Lan and R. F. Fox, Phys. Rev. A **43**, 646 (1991), and in recent work [55].
[52] G. S. Agarwal, Phys. Rev. A **51**, R2711 (1995), and references therein.
[53] V. Peřinová and A. Lukš, in *Progress in Optics XXXIII*, edited by E. Wolf (Elsevier, Amsterdam, 1994), p. 130.
[54] K. N. Alekseev and G. P. Berman, Zh. Éksp. Teor. Fiz. **88**, 968 (1985) [Sov. Phys. JETP **61**, 569 (1985)].
[55] K. N. Alekseev and D.S. Prijmak, Zh. Éksp. Teor. Phys. **113**, 111 (1998) [JETP (to be published)].